Quantum Shot Noise: From Schottky to Bell

M. Büttiker[a], P. Samuelsson[b], and E. V. Sukhorukov[a]

[a] Department of Theoretical Physics, University of Geneva, CH-1211 Geneva 4, Switzerland;
[b] Departmenet of Solid State Theory, Lund University, S-233 62 Lund, Sweden

ABSTRACT

Mesoscopic shot noise is not only probabilistic: it has features which reflect quantum mechanical entanglement. We discuss recent proposals of orbital entanglement generation and detection in mesoscopic coherent conductors. Orbital entanglement avoids the difficulty of detecting spin and leads to simpler structures. Orbital entanglement schemes invoke two two-particle sources. The index of the source plays the role of a pseudo-spin. The rotation of qubits can be implemented with beam-splitters or even just quantum point contacts. Entanglement is detected via violation of a Bell inequality. The necessary correlations can be extracted from shot noise measurements. Possible two particle sources are Cooper pairs emitted from superconductors or even simpler electron-hole pairs generated at tunnel contacts or generated dynamically with the help of oscillating potentials.

Keywords: Shot noise, two-particle Aharonov-Bohm effect, entanglement, Bell test

1. INTRODUCTION

For the last two decades the investigation of shot noise in small electrical conductors has been an important frontier in mesoscopic conductors.[1] Shot noise has been a tool to investigate properties of electrical conductors which are not accessible through conductance measurements.

Shot noise, investigated by Schottky,[2] almost a hundred years ago, is due to thermionic emission from the high-energy Boltzmann-like tail[3] of the Fermi distribution. Schottky's noise is *classical*, with a noise power proportional to the average current,

$$\langle(\Delta I)^2\rangle_\nu = 2e|\langle I\rangle| \tag{1}$$

In contrast, shot noise in mesoscopic conductors is a quantum mechanical phenomenon, a manifestation of the wave-particle duality. An electron incident on a scatterer can be either reflected or transmitted. The final state, however, is in both cases a carrier with a quantized charge, an electron. One the one hand, due to the probabilistic nature of quantum mechanical scattering, the same initial state (the electron approaching the barrier) can have several final states (reflection with amplitude r or transmission with amplitude t). This gives rise to a quantum *partition* noise[4–6] proportional to $T(1-T)$ where $T = |t|^2$ is the transmission probability. Since the average current will be proportional to transmission, one sees immediately that the quantum partition noise will be smaller than the Poisson result given by Eq. (1).

In this work we are interested in *entangled* states. In the simplest case of two composite systems, these are states which can not be written as a product of the wave functions of the two systems.[7–9] Best known are spin entangled states. Here our interest is in the entanglement of a different type. We consider *orbital* entanglement[10,11] which is generated if two or more contacts inject carriers into a conductor. In such a situation, we can not distinguish which electron has been injected where.[12] The shot noise correlations exhibit exchange interference terms.[12,13] In orbital entanglement the index of two injecting contacts plays the role of a pseudo-spin index.[11]

We focus on orbital entanglement since it seems much simpler to manipulate and detect than spin entanglement. Spins provide a natural qubit, and have been the focus of much of the recent efforts. We mention here only a few recent works which can serve as a guide to the literature.[14–17] The direct detection of spin entanglement requires a spin to charge conversion measurement. This is difficult since the detector needs to be capable to test spin polarization in an arbitrary direction. Alternatively, if the detector has a fixed polarization axis, spin needs

E-mail: Markus.Buttiker@physics.unige.ch

Fluctuations and Noise in Materials II, edited by Peter Svedlindh, Dragana Popovic, Michael B. Weissman, Proceedings of SPIE Vol. 5843 (SPIE, Bellingham, WA, 2005)
0277-786X/05/$15 · doi: 10.1117/12.609386

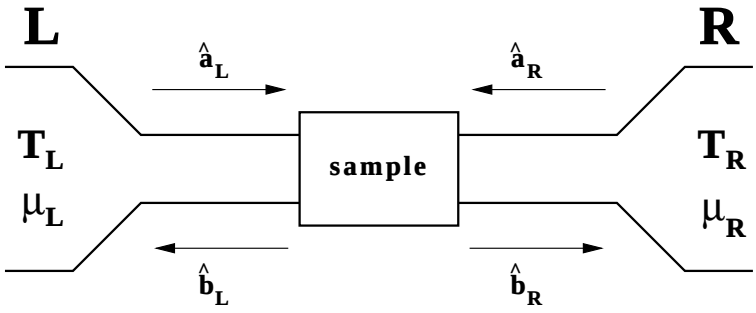

Figure 1. Two-probe conductor: incident states $\hat{a}_L, \hat{a}_R$ generate outgoing states $\hat{b}_L, \hat{b}_R$.

to be rotated before it impinges on a detector. In contrast, orbital entanglement can be detected with the help of beam splitters or even simply with the help of quantum point contacts. We emphasize and insist on considering not only the entanglement generation but also its detection, not only out of a desire for a complete description, but more fundamentally since in quantum mechanics the measurement process must be an integrated part in predictions of what can be observed.

2. CONDUCTANCE AND SHOT NOISE: TWO TERMINAL CONDUCTOR

We briefly restate some central results of the scattering theory of conductance and noise. This will help us to clarify the distinction between simple quantum partition noise and the information on entanglement in shot noise correlations.

A two-terminal conductor is shown in Fig. 1. Current amplitudes $\hat{a}_L$ and $\hat{a}_R$ describe waves incident from the left L and right R. Current amplitudes $\hat{b}_L$ and $\hat{b}_R$ describe amplitudes of out-going states. In general there are many channels (transverse modes) and $\hat{a}$ and $\hat{b}$ are vectors with as many components as there are transverse channels at the Fermi energy. Incoming and out-going states are related by the scattering matrix, $s_{RL} \equiv t$, $s_{LR} \equiv t'$, $s_{LL} \equiv r$, and $s_{RR} \equiv r'$. At zero temperature the conductance is

$$G = \frac{e^2}{h} Tr(t^\dagger t) = \frac{e^2}{h} \sum_n T_n \tag{2}$$

Here the trace Tr is over all transverse modes. The matrix $t^\dagger t$ is hermitian and can be diagonalized. Its eigenvalues are the transmission probabilities T_n. Note, that independent of the basis, the conductance is always expressed as a sum of transmission probabilities.

The shot-noise power is[6]

$$S = 2e\frac{e^2}{h}|eV|Tr(r^\dagger r t^\dagger t) = 2e\frac{e^2}{h}|eV| \sum_n T_n(1 - T_n) \tag{3}$$

At least in the eigen-channel basis, the shot noise is again only a function of transmission probabilities. In contrast, in multi-terminal conductors, shot noise can not be expressed in terms of single particle transmission probabilities, scattering-phases will appear in an explicite manner.

3. CONDUCTANCE AND SHOT NOISE: MULTI-TERMINAL CONDUCTOR

A multi-probe conductor is shown in Fig. 2. The scattering matrix of the conductor is composed of the matrices $s_{\alpha\beta}$ which describe the transmission/reflection amplitudes of carriers incident in contact β and transmitted/reflected into contact α. At zero temperature, the conductance matrix is,

$$G_{\alpha\alpha} = \frac{dI_\alpha}{dV_\alpha} = \frac{e^2}{h} Tr(N_\alpha - s^\dagger_{\alpha\alpha} s_{\alpha\alpha}), \;\; G_{\alpha\beta} = \frac{dI_\alpha}{dV_\beta} = -\frac{e^2}{h} Tr(s^\dagger_{\alpha\beta} s_{\alpha\beta}), \tag{4}$$

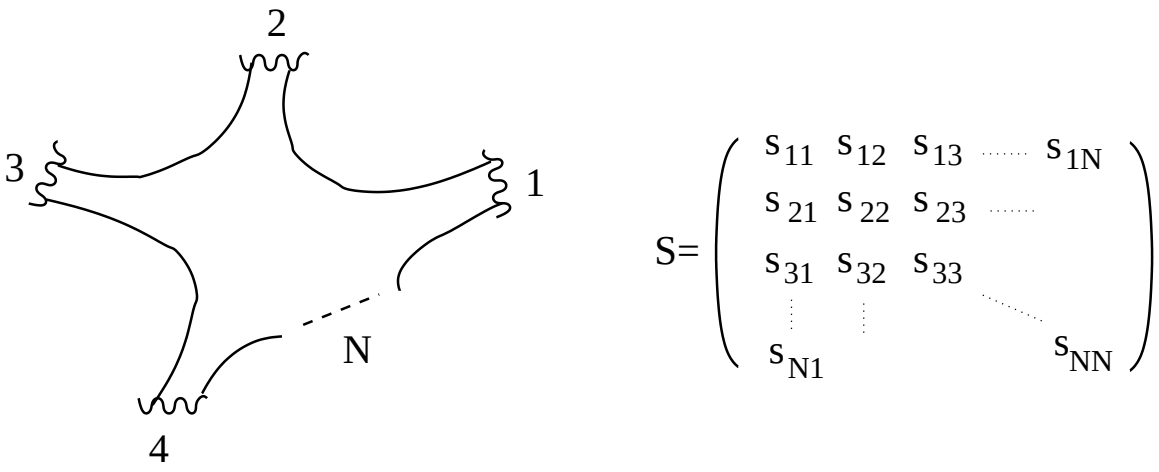

Figure 2. Multi-probe conductor and its scattering matrix.

where N_α is the number of quantum channels in contact α. We are interested in correlations of fluctuating currents with currents measured at different contacts $\alpha \neq \beta$,

$$S_{\alpha\beta} = 2 \int dt \langle \Delta\hat{I}_\alpha(t) \Delta\hat{I}_\beta(0) \rangle \tag{5}$$

In the zero-temperature limit, we find,[6,12]

$$S_{\alpha\beta} = 2\frac{e^2}{h} \int dE \mathrm{Tr} \left[B^\dagger_{\alpha\beta} B_{\beta\alpha} \right] , \;\; B_{\alpha\beta} = \sum_{\gamma=1}^{M} s_{\alpha\gamma} s^\dagger_{\beta\gamma} (f_\gamma - f_0) \tag{6}$$

Here f_γ is the Fermi distribution function of a contact at voltage V_γ and f_0 is the Fermi function of a contact that is grounded. Now if there is only one contact above ground $M = 1$ the correlation function still depends only on the scattering matrix multiplied with its hermitian conjugate, similar to the shot noise in a two-terminal conductor. But if $M \geq 2$ the correlation function contains now products of four scattering matrices in which none of the scattering matrices is the hermitian conjugate of the other. This implies that the correlation function depends on *phases of the scattering matrix elements*. The appearance of phases of scattering matrix elements, discussed already in Refs. 12, 13, is now central for what follows. We will show that such phases are connected to the fact that shot noise is a probe of two-particles processes. To illustrate this, we demonstrate first a novel type of Aharonov-Bohm effect,[12,13,18–20] which exists only due to two particle scattering processes. These phases are a manifestation of quantum non-locality and subsequently we link them to orbital entanglement.

4. TWO-PARTICLE AHARONOV-BOHM EFFECT

To high-light the role of phases of scattering matrix elements we search for a geometry in which the single-particle Aharonov-Bohm effect is absent and only the two-particle Aharonov-Bohm exists. This implies that none of the conductance matrix elements of such a multi-probe conductor depends on the Aharonov-Bohm flux, but shot noise correlations are oscillatory functions of flux. In optics, geometries in which time averaged intensities are feature-less but correlation functions exhibit an interference pattern have long been known. Such geometries are known as *intensity* interferometers,[21,22] in contrast to the better known amplitude interferometers, like the Mach-Zehnder or Michelson interferometer. The prime example is the stellar Hanbury Brown Twiss interferometer which was used to measure the angular diameter of stars. In fact the Hanbury Brown Twiss experiments set the stage for the development of quantum optics. A table top version of an optical intensity interferometer[22] is shown in Fig. 3. Photons are injected from 2 and 3. Contacts 5, 6 and 7, 8 are used to measure intensity correlations. The broken lines represent half-silvered mirrors. Each photon-path is singly connected, there are no single

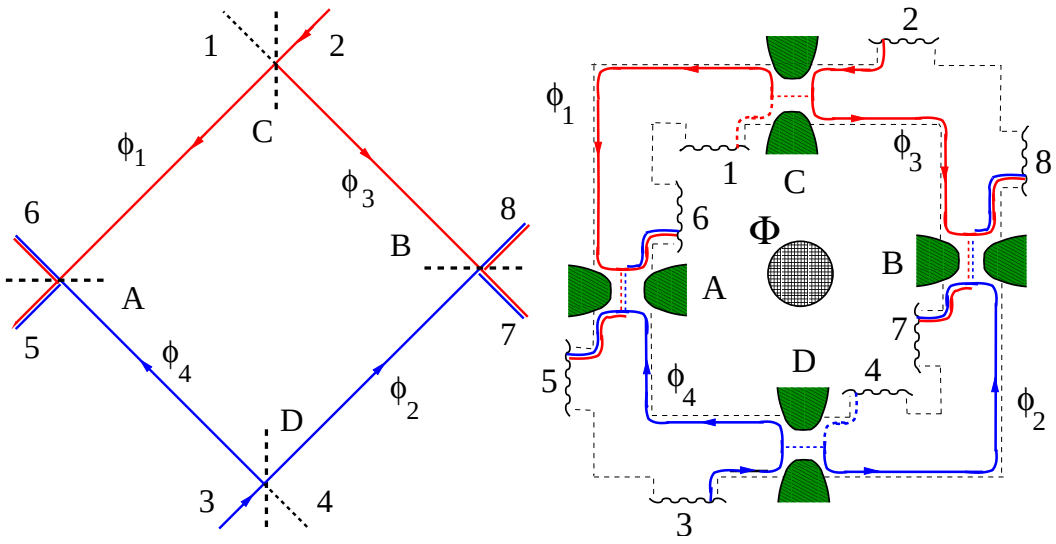

Figure 3. Left: Optical intensity interferometer: broken lines represent half-silvered mirrors. Photons incident from 2 and 3 end up in $5, 6, 7, 8$. There are no closed path and thus no single photon interference effects. Right: Electrical intensity interferometer: A Corbino disk with four quantum point contacts. Electrons incident from 2 or 3 end in contacts $5, 6, 7, 8$. There are no closed path and thus no single electron-interference effects. An Aharonov-Bohm flux penetrates the hole of the disk. After Ref. 18.

particle interfering alternatives. The time-averaged intensities are not sensitive to the phases ϕ_i accumulated in the traversal from one mirror to the other. However, the intensity correlations do depend on these phases. A topologically equivalent conductor,[18] is shown in Fig. 3. It is a Corbino disk[23] with four contacts on the outer perimeter and four contacts on the inner perimeter (not all these contacts are necessary for the demonstration of the two-particle Aharonov-Bohm effect). The role of mirrors is played by quantum point contacts (QPC) with transmission and reflection probabilities T_i and R_i, $i = A, B, C, D$. The arrows along the sample boundaries are the edge states of a two-dimensional electron gas in the $\nu = 1$ integral quantum Hall state. An Aharonov-Bohm flux penetrates the hole of the Corbino disk. Along a path, say along the outer edge from C to A electrons accumulate a kinetic phase ϕ_1 and due to the AB-flux a phase χ_1. We have $\chi_1 + \chi_3 - \chi_2 - \chi_4 = 2\pi\Phi/\Phi_0$ where $\Phi_0 = h/e$ is the single electron flux quantum. The scattering matrix elements of this conductor contain phases only in the form of a simple multiplicative phase factor. For instance the scattering matrix element for transmission from contact 2 to 5 is,

$$s_{52} = T_A^{1/2} e^{i(\phi_1+\chi_1)} T_C^{1/2}. \tag{7}$$

The conductance from contact 2 to 5 is $G_{52} = dI_5/dV_2 = -\frac{e^2}{h} T_A T_C$. All other elements of the conductance matrix are similarly independent of the AB-flux.

However, if we now evaluate the cross-correlations of currents, the noise-spectra do depend on flux. According to Eq. (3) we have to evaluate

$$S_{58} = -2\frac{e^2}{h} \int dE |s_{52}^* s_{82} + s_{53}^* s_{83}|^2 (f - f_0)^2 \tag{8}$$

to find the current-cross correlation between contacts 5 and 8. For example for $T_A = T_B = T_C = T_D = 1/2$ we find,[18]

$$S_{58} = -\frac{e^2}{4h} |eV| \left[1 + \cos\left(\phi_1 + \phi_2 - \phi_3 - \phi_4 + 2\pi \frac{\Phi}{\Phi_0} \right) \right] \tag{9}$$

which exhibits a simple oscillation due to the AB-flux.

The flux dependence in the current cross-correlation is a consequence of the fact that the correlation probes two-particle processes.[18] Specifically in our interferometer, the contribution to the correlation come from

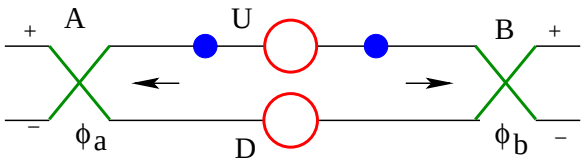

Figure 4. Schematics of the orbital entangler arrangement: two two-particle sources (circles emit particles towards detectors A and B which rotate the qubit with phase angles ϕ_a and ϕ_b.

processes in which a particle is emitted from contact 2 towards 5 and from contact 3 towards 8. This process is indistinguishable from the emission of a particle from 2 towards 8 and from 3 towards 5. The amplitudes of these two two-particle processes have to be added. But the two two-particle processes now do encircle the AB-flux!!

5. ORBITAL ENTANGLEMENT

We now discuss an orbital entanglement scheme and subsequently return to the electron intensity interferometer. Figure 4 demonstrates schematically the principle of an orbital entangler. There are two sources (red circles in Fig. 4) denoted U (up) and D (down) which emit two particles, one to A and one to B. The two particles emitted by a source do not necessarily have to be identical. But it is important that both sources emit the same type of particle to the left side and same the type of particles to the right. In our initial work we used a superconductor as a two particle source.[11] Later Beenakker et al.[24,25] pointed to sources which emit electrons-hole pairs. The two particle wave function generated by these two sources is of the form

$$\Psi = \frac{1}{\sqrt{2}}\left[\Psi_U(A)\Psi_U(B) + \Psi_D(A)\Psi_D(B)\right] \tag{10}$$

and describes a state that is entangled with respect to the source indices U and D. The spatial separation of the two two-particle sources is only desirable for enhanced control but it is not a fundamental requirement. To analyze the state, we send it onto analyzers A and B which can rotate the state through an angle ϕ_a and ϕ_b. One reason that orbital entanglement schemes are simpler than spin entanglement is due to the fact that simple beam-splitters rotate orbitally entangled states.

Theoretically we can verify that a state is entangled by constructing it and by evaluating an entanglement measure. Experimentally, we can not (typically) directly investigate the state but must rely on other criteria to find out whether we have an entangled state or not. An inequality developed by Bell[9,26] can serve this purpose. Originally developed to separate quantum mechanical non-locality from classical local states, here, the purpose is not to test fundamental aspects of quantum mechanics but simply to use the inequality as a test for entanglement.[11,27–29] It is not the only possible criteria but the Bell correlations which enter the inequality are closely related to intensity correlations. We will now show that the electron intensity interferometer[18] in fact contains already all these elements. A Bell test[26] is based on the "equal-time" correlations

$$E(\theta_A,\theta_B) = \frac{\langle (I_{A+} - I_{A-})(I_{B+} - I_{B-})\rangle}{\langle (I_{A+} + I_{A-})(I_{B+} + I_{B-})\rangle} \tag{11}$$

where $I_{i\sigma}$ are intensities (currents) at contacts $i\sigma$, $i = A, B$, $\sigma = \pm$. A classical system has

$$S_B = |E(\theta_A,\theta_B) - E(\theta'_A,\theta_B) + E(\theta_A,\theta'_B) + E(\theta'_A,\theta'_B)| \leq 2 \tag{12}$$

On the other hand, if there exist angles $\theta_A, \theta_B, \theta'_A, \theta'_B$ such that S_B exceeds 2 we know the state is entangled.

6. ELECTRON-HOLE ENTANGLEMENT IN LOW FLUX LIMIT

We now return to the intensity interferometer of Fig. (2) to discuss its non-local properties. We first consider the limit of a very asymmetric (tunnel limit) interferometer. We take the reflection probability R_C at C for carriers incident from 2 and the transmission probability T_D for carriers incident form 3 to small, $R_C = T_D = R \ll 1$.

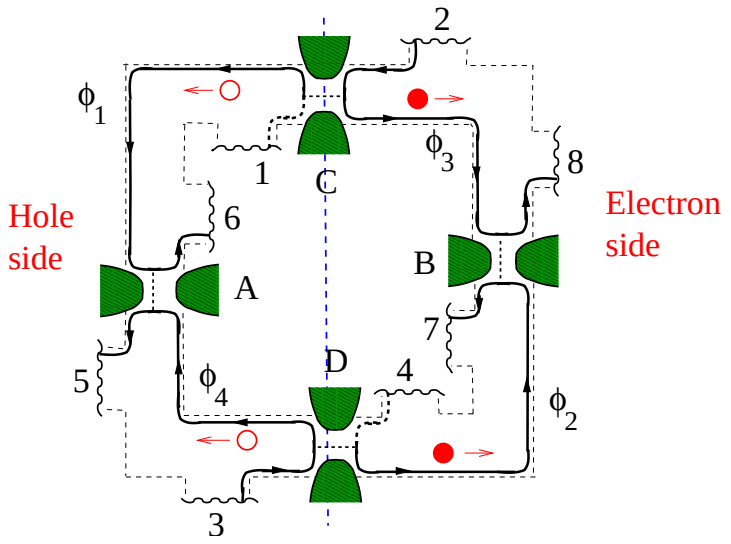

Figure 5. Electron-hole pairs in the intensity electron interferometer: quantum point contact C weakly reflects electrons, contact D weakly transmits electrons. Each reflection event at C and each transmission event at D leaves behind a hole. After Ref. 18.

As a consequence electrons incident from 2 are very rarely reflected towards B and the missing electrons on the left side of QPC C can be viewed as a hole (see Fig. 5). Similarly electrons from 3 are only very rarely transmitted and through QPC D and the missing electron in the reflected stream can again be viewed as a hole. Thus each reflection event at C and each transmission event at D creates an electron-hole pair. This is similar to the proposal of Beenakker et al.[24] except that here the two sources are spatially separated and thus individually controllable. On the left side of our interferometer excitations are holes in a ground state with Fermi energy $\mu = eV$ and excitations on the right side are electrons in a ground state with Fermi energy 0. (We take the equilibrium Fermi energy to be at $E = 0$). The incident state is a many particle electron state with energies in the range $0 < E < eV$,

$$|\Psi_{in}\rangle = \prod_{0<E<eV} c_2^\dagger(E) c_3^\dagger(E)|0\rangle \tag{13}$$

We next introduce creation (and annihilation) operators in the out-going regions of the QPC's C and D,

$$c_2^\dagger = t_C c_{2A}^\dagger + r_C c_{2B}^\dagger\,; \;\; c_3^\dagger = r_D c_{3A}^\dagger + t_D c_{3B}^\dagger \tag{14}$$

In terms of these operators we obtain for the out-going state to lowest order in the reflection probability,[18]

$$|\Psi\rangle = |\bar{0}\rangle + \sqrt{R}\int_0^{eV} dE \left[c_{3B}^\dagger c_{3A} - c_{2B}^\dagger c_{2A}\right]|\bar{0}\rangle \tag{15}$$

This is an *orbitally* entangled electron-hole state. It is important that here $|\bar{0}\rangle$ is the equilibrium state mentioned above with the voltage drop eV across the QPC's C and D incorporated. It is the introduction of this tunneling ground state[18] which permits to describe the excitations as electron-hole pairs.

7. ENTANGLEMENT TEST

We now demonstrate that the state Eq. (15) violates the Bell inequality. As above we consider the tunnel limit and set $\phi_1 + \phi_2 - \phi_3 - \phi_4 + 2\pi\Phi/\Phi_0 = 2\pi$. In the orbital entangler set-up the two detector QPC's A and B "'rotate" the qubit. The scattering matrices of these two QPC's are

$$S_{A/B} = \begin{pmatrix} \cos\theta_{A/B} & -\sin\theta_{A/B} \\ \sin\theta_{A/B} & \cos\theta_{A/B} \end{pmatrix} \tag{16}$$

which introduces the angles needed in the Bell test. With these specifications we find for the shot noise current correlations

$$S_{58} = S_{67} = -S_0 P_{++}\,; \;\; S_{57} = S_{68} = -S_0 P_{+-} \tag{17}$$

where $S_0 = -(4e^2/h)|eV|R$, and

$$P_{\sigma,\sigma'} = (1 + \sigma\sigma' \cos[2(\theta_A - \theta_B)])/4 \tag{18}$$

with $\sigma = \pm, \sigma' = \pm$. Here P has just the form that one would expect in a Bell test of a spin entangled state. Eq. (18) permits to obtain the Bell correlation, $E(\theta_A, \theta_B) = P_{++} + P_{--} - P_{+-} - P_{-+}$. Note, that the Bell test requires an equal-time correlation, whereas the quantity that is presently accessible in a shot noise measurements is the zero-frequency noise. However, in the low flux limit considered here, the cross-correlation is just an equal time measurement run over a long time.[11] Only co-incident current pulses will contribute to the correlation. Such correlated current pulses must necessarily come from the electron-hole pair that was generated in a correlated event. Subsequent pairs are generated with a typical time interval $\tau \sim \hbar/eVR$ (remember $R << 1$) which is long compared to a correlation time of an electron-hole pair $\tau \sim \hbar/eV$.

Alternatively we can calculate the joint detection probability Eq. (18) directly using the state Eq. (14). The tunnel limit represents thus a very transparent situation. Since the electron-hole pairs are well separated in time, there is in this limit also the possibility to dynamically manipulate the entangled state during its transfer to the detector. Therefore, the entanglement we have in the tunnel limit is likely "'useful".

We remark that if dephasing[11, 30, 31] is introduced in our intensity interferometer, through reduction of the off-diagonal elements of the density matrix[30] in the qubit space, the Bell parameter becomes $S_B^{max} = 2\sqrt{1 + \gamma^2 \cos^2 \phi_0}$. Here γ is the dephasing parameter that multiplies the off-diagonal density matrix elements, $0 < \gamma < 1$. Importantly the Bell inequality can be violated independent of the degree of (this type[32]) of dephasing. Returning to the two particle AB-effect we find that γ determines the visibility of the two-particle AB-effect. This again demonstrates the close link between the two-particle AB-effect and entanglement in our intensity interferometer.

8. ELECTRON-ELECTRON ENTANGLEMENT

The two-particle Aharonov-Bohm effect exists not only in the tunnel limit but in fact for arbitrary settings of transmission probabilities in the intensity interferometer.[18] For "large" transmission probabilities $T_C \approx T_D \approx 1/2$ the electron-hole picture is, however, not any longer useful. We return to an electron picture only. The full many electron state is a product state. Elastic scattering performs only a linear transformation on the state and does thus not change this fact. However, the statement that the full state is a product state and thus not entangled is entirely irrelevant.[24] What counts is the state in two regions A and B and not the full state. Indeed, we find that also in the highly transparent interferometer a Bell inequality can be violated. The essential point is that we probe in this limit only two particle properties of the state. We have termed this entanglement through "post selection". To treat the case of a (nearly) symmetric intensity interferometer we start from the Glauber joint detection probability, and find[18]

$$P_{\alpha\beta} \propto \langle b_\beta^\dagger(t) b_\alpha^\dagger(t) b_\alpha(t) b_\beta(t)\rangle = (h^2/e^2)[(1/2\tau_c) S_{\alpha\beta} + I_\alpha I_\beta] \tag{19}$$

where $\tau_C = \hbar/eV$ and I_α, I_β are average currents. Using the scattering matrix for the average currents permits to write

$$\langle b_\beta^\dagger(t) b_\alpha^\dagger(t) b_\alpha(t) b_\beta(t)\rangle = (eV)^2 |s_{\alpha 3} s_{\beta 2} - s_{\alpha 2} s_{\beta 3}|^2 \tag{20}$$

Apart from the factor $(eV)^2$, the right hand side is just the two-particle transmission probability for two electrons injected simultaneously at contacts 2 and 3. For the maximum Bell parameter we find

$$S_B^{max} = 2\sqrt{1 + \cos^2 \phi_0} \tag{21}$$

where $\phi_0 = \phi_1 + \phi_2 - \phi_3 - \phi_4 + 2\pi\Phi/\Phi_0$. Clearly the maximal Bell parameter exceeds 2, signaling entanglement. The origin of this two-electron entanglement can be understood as follows: The anti-bunching of electrons implies that no two electrons can be emitted simultaneously from a single reservoir. As a consequence, only the process

where one electron is emitted from the source C and one from D can lead to a joint detection in A and B. Since the paths of these two particles can not be distinguished, the corresponding state is orbitally entangled.

For the symmetric interferometer, electron-electron entanglement appears only on the short time scale $\tau_C = \hbar/eV$. To make use of the entanglement of this state is thus likely more difficult and might make this a "less useful" entanglement.

We conclude with a remark on related work on Bell inequalities in mesoscopic conductors. Chtchelkatchev et al.,[28] Faoro et al.[33] and Lebedev et al.[29] formulate Bell inequalities in mesoscopic conductors in terms of the charge transfered $Q_\alpha(t,\tau_m) = \int_0^{\tau_m} dt I_\alpha(t)$ during a certain measurement time τ_m. In the tunneling limit,[28,29] with a proper choice of measurement time, the resulting Bell inequality is independent of this time. However, in the high flux limit, the Bell inequality depends on the measurement time. The same dependence on the measurement time was found for Bell inequalities formulated directly in terms of current correlators.[29] While it is possible to pump charges one by one, counting charges similar to counting photons with a detector, is thus far not possible. For quasi-particles the equal-time information (equal on the scale of the correlation time τ_C) is related to long-time measurements in a simple way, as exemplified by Eqs. (19,20).

9. DYNAMIC GENERATION OF QUASI-PARTICLE ENTANGLEMENT

The orbital entanglers which we have presented thus far are stochastic. The emission of pairs of particles (in the electron-hole limit) is Poissonian. It is clearly desirable to find ways to generate entangled states in a more controlled way. In classical machines, computation is a time-dependent process with elementary steps often controlled by a master-clock.[34] Idealy it should be possible to use the signal from the master-clock to produce entanglement on command, once per clock-cycle.

As a first step towards time-controlled quasiparticle entanglement, two of us,[35] have analyzed a dynamic scheme to generate and detection of orbitally entangled electron-hole pairs in a mesoscopic conductor. Pairs are generated by electrical potentials that are varied periodically and adiabatically at two spatially separated regions in the conductor . A possible dynamic intensity interferometer is shown in Fig. 6. The oscillating potential excites electron-hole pairs, for instance through the modulation of the voltages at two gates which span the conduction channel. Alternatively two quantum point contacts can be used and the voltage to one of the gates creating the contact can be modulated. To guide the electron-hole pairs away from the region underneath the gates we again consider a two-dimensional electron gas in the integer quantum Hall state $\nu = 1$. The scheme follows the general prescription given in Sect. V. The generated electron-hole pairs are orbitally entangled with respect to the two regions of emission. The emitted quasi-particles are detected in electronic reservoirs, all kept at zero bias, connected to the conductor.

This structure is even easier to fabricate than the stochastic orbital entangler shown in 3. Only two interior contacts are needed. Our scheme bears some resemblance to quantum pumping[36–39] but due to the chiral nature of the geometry *no net electrical current per clock-cycle is generated*. Instead the excited quasi-particles give rise to electrical current noise. Shot noise in the absence of dc-current has recently been measured in an experiment which excites electron-hole pairs with the help of an oscillating contact potential.[40]

In our work[35] we have focused on the adiabatic limit. In this limit the oscillation period $\tau = 2\pi/\omega$ is long not only compared to the transmission and reflection times of carriers underneath the gate but also compared to the propagation time of carriers from the gates to the detector contacts. In this limit the amplitudes for scattering between the reservoirs 1 to 4 are independent on energy on the scale of the clock frequency ω. The temperature is taken much smaller than $\hbar\omega$. Due to the oscillating potentials at C and D, electrons incident from the reservoirs 1 to 4 can absorb or emit one or several quantas of energy $\hbar\omega$ before propagating out to the reservoirs again.[34] In this Floquet picture,[37,38] the scattering in both energy and real space can be described by scattering matrices

$$S_{C/D}(E_n, E) = \begin{pmatrix} r_{C/D}(E_n, E) & t'_{C/D}(E_n, E) \\ t_{C/D}(E_n, E) & r'_{C/D}(E_n, E) \end{pmatrix} \tag{22}$$

where e.g. $t_C(E_n, E)$ is the amplitude for an electron incoming at energy E from left towards C to be transmitted to the right at energy $E_n = E + n\hbar\omega$. The dependence of the scattering amplitudes on $V_{C/D}(t)$ is determined

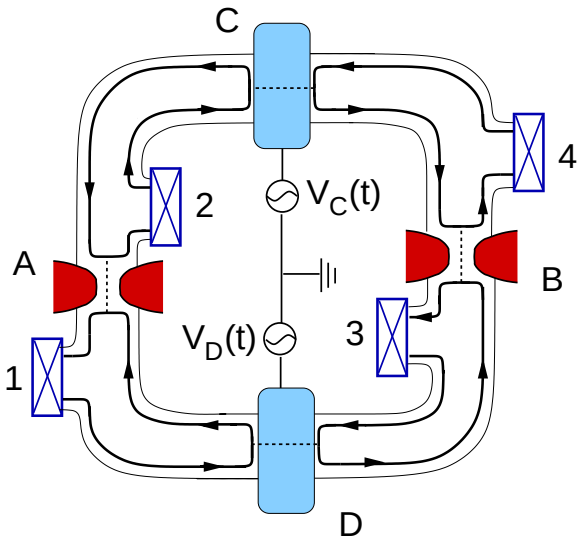

Figure 6. Dynamic entanglement generation: Intensity geometry in the quantum Hall regime. Transport takes place along a single edge state (thick black line) in the direction shown by the arrows. The potentials $V_C(t)$ and $V_D(t)$ at C and D are adiabatically and periodically modulated in time, creating electron-hole pairs propagating towards reservoirs 1 to 4. The static point contacts at A and B work as controllable beam-splitters. After 35.

by the properties of the scattering potential in the regions C and D. Here we only work with the scattering amplitudes themselves to keep maximum generality.

We also focus on the limit of weakly oscillating potentials, $V_{C/D}(t) = V_{C/D} + \delta V_{C/D}\cos(\omega t + \phi_{C/D})$, with $\delta V_{C/D}$ so small that only the amplitudes to absorb or emit one quanta (proportional to $\delta V_{C/D}$) need to be taken into account. The relevant scattering amplitudes are then e.g. $t_D \equiv t_D(E,E)$ and $\delta t_D^{\pm} = \delta t_D \exp(\pm i\phi_D) \equiv t_D(E_{\pm 1}, E)$, with $\delta t_D = \delta V_D(\partial t_D/\partial V_D)/2$, and similar for the other amplitudes. In this low frequency, low amplitude regime we are able to carry out the entire program: the calculation of the orbitally entangled quantum states and the detection via violation of a Bell inequality from shot noise correlation spectra.

The state of the particles emitted from the two regions C and D can be constructed from the many-body state of the electrons incident from the reservoirs 1 to 4, (suppressing spin) $|\Psi_{in}\rangle = \prod_{j=1}^{4}\prod_E a_j^\dagger(E)|0\rangle$, where $|0\rangle$ is the true vacuum and $a_j^\dagger$ creates an electron at energy E, incident from reservoir j. Introducing operators, $b_{AC}^\dagger(E)$ creating an outgoing electron at energy E at contact C propagating towards contact A, we can relate the b-operators to the a-operators at C as

$$\begin{pmatrix} b_{AC}(E) \\ b_{BC}(E) \end{pmatrix} = \sum_{n=0,\pm 1} S_C(E, E_n) \begin{pmatrix} a_2(E_n) \\ a_4(E_n) \end{pmatrix} \tag{23}$$

and similarly at D. Inserting these relations into $|\Psi_{in}\rangle$ and expanding to first order $\delta V_{C/D}$, we find the state outgoing from C and D in terms of the b-operators as

$$|\Psi_{out}\rangle = |\bar{0}\rangle + \int_{-\hbar\omega}^{0} dE \left(|\Psi_{out}^C(E)\rangle + |\Psi_{out}^D(E)\rangle\right) \tag{24}$$

with

$$|\Psi_{out}^C(E)\rangle = \sum_{\alpha,\beta=A,B} f_{\alpha\beta}^C b_{\alpha C}^\dagger(E_1) b_{\beta C}(E)|\bar{0}\rangle \tag{25}$$

where $f_{AA}^C = \delta r_C^+ r_C^* + \delta t_C'^+ t_C'^*$, $f_{BB}^C = \delta t_C^+ t_C^* + \delta r_C'^+ r_C'^*$, $f_{AB}^C = \delta r_C^+ t_C^* + \delta t_C'^+ r_C'^*$, $f_{BA}^C = \delta t_C^+ r_C^* + \delta r_C'^+ t_C'^* = -e^{-2i\phi_C}(f_{AB}^C)^*$ and $|\Psi_{out}^D\rangle = |\Psi_{out}^C\rangle$ with $C \to D$. The ground state in terms of outgoing operators is $|\bar{0}\rangle =$

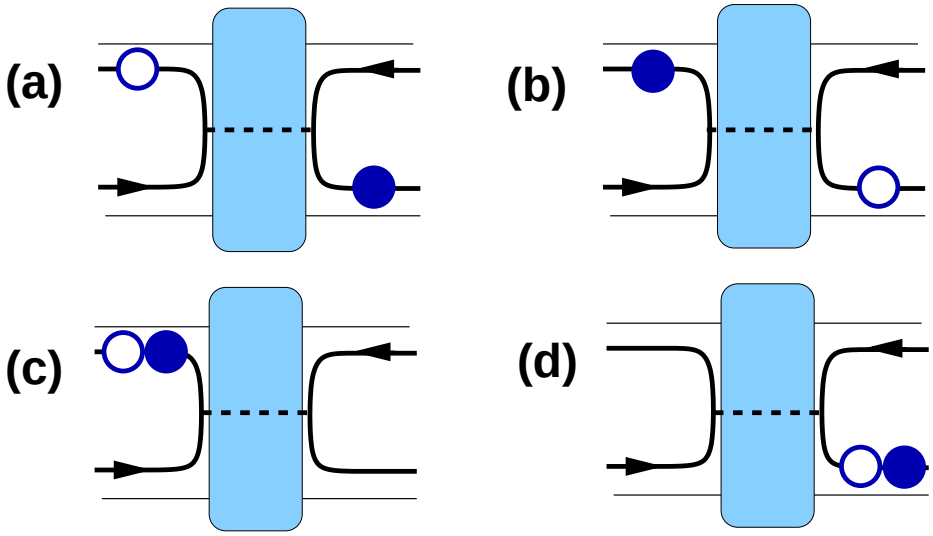

Figure 7. The four different electron-hole pair emission processes at C: In the two upper processes, the pair is split and (a) the electron is emitted towards B and the hole towards A, or (b) the electron towards A and the hole towards B. In the two lower processes, both quasi-particles are emitted towards (c) A or (d) towards B. The same processes occur at D. After Ref. 35.

$\prod_E b^\dagger_{AC}(E)b^\dagger_{BC}(E)b^\dagger_{AD}(E)b^\dagger_{BD}(E)|0\rangle$. Each term in Eq. (25) contains an operator product $b^\dagger_{\alpha C}(E_1)b_{\beta C}(E)$ acting on the ground state $|\bar{0}\rangle$, describing the destruction of one electron at an energy $-\hbar\omega < E < 0$ below the Fermi surface, i.e. the creation of a hole, and the creation of an electron at energy $0 < E_1 < \hbar\omega$ above (in leads αC and βC respectively). The effect of the weak potential oscillations is thus to create electron-hole pair excitations out of the ground state.[41] The four different scattering processes at each contact C and D are pictured schematically in Fig. 7.

The state in Eq. (24) is orbitally entangled. It is a linear superposition of electron-hole pair wave packets emitted at C and D, i.e. the contact indices C and D form an orbital two-level system, or qubit. In first quantization for identical scattering amplitudes at C and D, the excitation out of the ground state $|\bar{0}\rangle$ in Eq. (24) can be written $(|CC\rangle + |DD\rangle) \otimes |\bar{\Psi}\rangle$, where $|CC\rangle + |DD\rangle$ is an orbitally entangled triplet state and $|\bar{\Psi}\rangle$ contains all additional properties of the state, e.g. energy dependence and quasi-particle character. We note that the emitted wave-packets contain quasi-particles in the energy range $\hbar\omega$. The clock frequency thus, in this respect, plays the same role as the applied voltage in the entanglement schemes in e.g. Refs. 11, 18, 24.

The entanglement is detected via violation of a Bell inequality using noise correlations similar to the stochastic intensity interferometer discussed above. The noise properties of pumped mesoscopic conductors are the properties of several works..[38,39] The cross-correlation between the currents $i = 1, 2$ and $j = 3, 4$, averaged over the time difference t', is defined as

$$S_{ij}(t) = 2e \int dt' \langle \Delta I_i(t + t'/2)\Delta I_j(t - t'/2)\rangle \tag{26}$$

with $\Delta I_j(t) = I_j(t) - \langle I_j(t)\rangle$. In contrast to the intensity interferometers discussed above this spectrum is time-dependent. The zero-frequency part of this spectrum is found to be, for e.g. reservoirs 1 and 3

$$S^{dc}_{13} = \frac{e^2}{\tau}\left[|f^C_{AB}\sin\theta_A \sin\theta_B + f^D_{AB}\cos\theta_A\cos\theta_B|^2 + |f^C_{BA}\sin\theta_A\sin\theta_B + f^D_{BA}\cos\theta_A\cos\theta_B|^2\right] \tag{27}$$

This expression has a simple physical explanation.[35] The first term in the bracket in Eq. (27) is the amplitude for an emitted electron-hole pair from C or D to split, with the electron ending up in reservoir 1 and the hole in 3. The second term is just the amplitude for the opposite process, the electron detected in 3 and the hole in 1.

The other correlators are found similarly. We note that only the scattering processes where the pair splits [(a) and (b) in Fig. 7] contribute to the leading order cross-correlators.[11]

Considering for simplicity the case where the two scattering potentials at C and D are equal, i.e. $t_C = t_D = t$ etc, up to the pump phases $\phi_{C/D}$, one can write

$$S_{13}^{dc} = S_0 \left[\cos^2\theta_A \cos^2\theta_B + \sin^2\theta_A \sin^2\theta_B + 2\gamma \cos\theta_A \cos\theta_B \sin\theta_A \sin\theta_B\right] \tag{28}$$

with $S_0 = (e^2/\tau)|\delta r t^* + \delta t' r'^*|^2$, $\gamma = \cos\varphi \cos(\phi_C - \phi_D)$ and $S_{24}^{dc} = S_{13}^{dc}$ and $S_{14}^{dc} = S_{23}^{dc} = S_{13}^{dc}(\theta_B \to \theta_B + \pi/2)$. Here φ is an overall phase containing possible scattering phases of contacts A and B and phases due to propagation along the edge states, including Aharonov-Bohm phases. The noise correlator is proportional to $|\delta r t^* + \delta t' r'^*|^2$, i.e. proportional to δV^2. The last term in the bracket, the interference term, is proportional to $\cos(\phi_C - \phi_D)$, i.e. the interference term is maximized for the two pumping potentials in phase. Due to the phase-dependent term $\cos\varphi$, the noise correlators show a two-particle Aharonov-Bohm effect, similarly to Ref. [18, 19].

A Bell Inequality[9, 26] can be formulated in terms of the probability to jointly detect[11, 18] one quasiparticle at A and one at B during a clock-cycle. This probability is formally defined as $P_{ij} = \int_0^\tau dt dt' P_{ij}(t,t')$ with $P_{ij}(t,t') = P_{ij}^{eh}(t,t') + P_{ij}^{eh}(t,t') + P_{ij}^{ee}(t,t') + P_{ij}^{hh}(t,t,')$ and e.g.

$$P_{ij}^{eh}(t,t') \propto \langle c_i^{e\dagger}(t) c_j^{h\dagger}(t') c_j^h(t') c_i^e(t)\rangle. \tag{29}$$

The quasiparticle operators are defined as $c^e(t) = \int_0^\infty dE \exp(iEt/\hbar) c(E)$ and $c^h(t) = \int_{-\infty}^0 dE \exp(-iEt/\hbar) c^\dagger(E)$. Evaluating the joint detection probability, we find to leading order in δV that $P_{ij} \propto S_{ij}^{dc}$, as anticipated from the discussion below Eq. (27). One can thus formulate the Bell inequality in terms of the period-averaged, zero-frequency noise.[11, 18, 28] Choosing an optimal[11] set of scattering angles $\theta_A, \theta'_A, \theta_B, \theta'_B$, we arrive at the Bell Inequality $2\sqrt{1+\gamma^2} < 2$ which is maximally violated for $\phi_D - \phi_C = \varphi = 0 \bmod 2\pi$. We note that dephasing can be treated in the same way as in Ref. [11, 30].

So far we considered the limit of weak amplitude potential oscillations, where only one quanta $\hbar\omega$ is absorbed or emitted by the scattering electrons in regions C and D. Relaxing this assumption, for arbitrary strong potential modulations, it is no longer possible to write the state emitted by contacts C and D as an excitation of a single electron-hole pair out of the ground state. Instead, the state can be written as a linear superposition of excitations of multiple electron-pairs, describing a complicated multi-particle entanglement. Moreover, while the amplitude of the weak potential state oscillates with the single frequency ω, the strong potential state can have a complicated time-dependence with a sum of amplitudes with oscillation frequencies $n\hbar\omega$. A calculation of the joint detection probability P_{ij} shows that it can in the general case, i.e. without considering particular scattering potentials, not be expressed in terms of the noise cross correlator in Eq. (28). This is a consequence of the complicated time-dependence of the emitted state. Moreover, averaging the time-dependent probability $P_{ij}(t,t')$ over a time-scale much longer than τ gives a P_{ij} dominated by a quasiparticle current product term, which makes a violation of the Bell Inequality impossible..[28, 29] Clearly in the strong amplitude case a properly adapted detection scheme has to be developed.

10. OPTIMAL DYNAMICAL ENTANGLEMENT PUMP

Recent work by Beenakker, Titov and Trauzettel[42] investigates the optimization of a dynamical quantum entanglement pump. How close can one get to the generation of one entangled electron-hole pair per pump cycle? They investigate a quantum entanglement pump in the limit of large potentials. It is well known that pumps can transfer electrons one by one.[43] On the other hand it is also clear that the orbital entanglement scheme of Fig. (4) does not work in the limit of deterministic two particle production. Therefore, there exist conditions for which the pump is most efficient. The efficiency of the pump is defined with the help of probabilities w_{nm}^{eh} per unit time that the pump generates an electron with energy $E + n\hbar\omega$ to the left and hole with energy $E - m\hbar\omega$ to the right multiplied by the entanglement entropy ϵ_{nm}^{pq}

$$\epsilon = \sum_{E_n > E_F, E_m < E_F} [w_{nm}^{eh} \epsilon_{nm}^{eh} + w_{mn}^{he} \epsilon_{mn}^{he}]. \tag{30}$$

For a spin-independent 2×2-scattering matrix, the electron-hole pair is maximally entangled $\epsilon_{nm}^{eh} = \epsilon_{mn}^{he} = 1$ and the average entanglement production per cycle is[42]

$$\epsilon = \sum_{E_n > E_F, E_m < E_F} [w_{nm}^{eh} + w_{mn}^{he}]. \tag{31}$$

The probabilities w_{mn}^{he} are evaluated by projecting the state of the pump on an electron-hole pair with energy $E + n\hbar\omega$ to the left (A) and $E - m\hbar\omega$ to the right (B) with either spin up or down,

$$\mathcal{P}_{nm}^{eh} = \sum_{\sigma,\sigma'=\uparrow,\downarrow} \alpha_{\sigma,\sigma'} b_{A\sigma}^{\dagger} b_{B\sigma'}^{\dagger} |0> . \tag{32}$$

The coefficients $\alpha_{\sigma,\sigma'}$ of the projected states form a $2x2$ matrix from which one can determine[42] $w_{mn}^{he} = Tr\alpha\alpha^{\dagger}$. The probability Eq. (31) can b written as

$$\epsilon = P_0^{\uparrow} P_1^{\downarrow} + P_0^{\downarrow} P_1^{\uparrow}, \tag{33}$$

where P_{ν}^{σ} is the probability that ν spatially separated electron-hole pairs are generated in a given cycle.[42] For a spin-independent quantum pump we have $0 \leq P_1^{\uparrow} = P_1^{\downarrow} \leq 1 - P_0^{\uparrow} = 1 - P_0^{\downarrow} \leq 1$ and it follows that

$$\epsilon \leq 2P_0^{\sigma}(1 - P_0^{\sigma}) \leq 1/2 \tag{34}$$

The maximal entanglement[42] $\epsilon_{max} = 1/2$ of half a bit per cycle is reached for $P_0^{\uparrow} = P_0^{\downarrow} = P_1^{\uparrow} = P_1^{\downarrow} = 1/2$. Form this result it is clear that a deterministic spin independent pump produces no entanglement, since $P_0^{\sigma} = 0$ implies $\epsilon = 0$. This analysis demonstrates that as much as one Bell pair per two cycles can be generated by a spin-independent pump.

11. CONCLUSIONS

In this work we have discussed aspects of shot noise in small coherent conductors related to a profound paradigm of quantum mechanics known as entanglement. We have emphasized that a certain type of entanglement, orbital entanglement, is directly related to shot noise correlations. Such orbital entanglement is present when we inject carriers from two different contacts (or even just from two quantum channels). Examples are electron-electron pairs emitted from two superconducting-normal contacts, stochastic electron-hole generation at tunneling contacts or dynamically generated electron-hole pairs in "quantum pumps". An interesting signature is a two-particle Aharonov-Bohm effect for which we have proposed a geometry which permits an unambiguous demonstration. We have emphasized the generality of such orbital entanglement schemes and are convinced that it provides a road map for the invention of additional "orbital entanglers".

ACKNOWLEDGMENTS

This work is supported by the Swiss National Science Foundation and the program on Materials with Novel Electronic Properties (MaNEP).

REFERENCES

1. Ya. M. Blanter and M. Büttiker, "Shot Noise in Mesoscopic Conductors", Phys. Rep. **336**, 1-166, (2000).
2. W. Schottky, "Ueber spontane Stromschwankungen in verschieden Elektrizitẗsleitern", Ann. Phys. (Leipzig) **57**, 541 -567 (1918).
3. C. Schönenberger, S. Oberholzer, E.V. Sukhorukov, H. Grabert, "Shot Noise in Schottky's Vacuum Tube", (unpublished). cond-mat/0112504
4. V. A. Khlus, "Current and voltage fluctuations in microjunctions of normal and superconducting metals", Sov. Phys. JETP **66**, 1243 -1249 (1987).
5. G. B. Lesovik, "Excess noise in quantum point contacts", JETP Lett. **49**, 592 - 594 (1989).

6. M. Büttiker, "Scattering theory of thermal and excess noise in open conductors", Phys. Rev. Lett. **65**, 2901 - 2904 (1990).
7. E. Schrödinger, "Die gegenwärtige Situation in der Quantenmechanik", Naturwissenschaften, **23**, 807 -812, (1935); **23**, 844 -849 (1935).
8. A. Einstein, B. Podolsky and N. Rosen, "Can Quantum-Mechanical Description of Physical Reality Be Considered Complete?" Phys. Rev. **47**, 777 - 780, (1935); D. Bohm and Y. Aharonov, "Discussion of Experimental Proof for the Paradox of Eisntein, Rosen, Padolsky", *ibid* **108**, 1070 - 1076, (1957).
9. J. Bell, "On the Einstein-Podolsky-Rosen paradox", Physics **1**, 195 - 200 (1964).
10. M. A. Horne, A. Shimony, and A. Zeilinger, "Two-particle interferometry", Phys. Rev. Lett. **62**, 2209-2212, (1989).
11. P. Samuelsson, E.V. Sukhorukov, and M. Büttiker, "Orbital Entanglement and Violation of Bell Inequalities in Mesoscopic Conductors", Phys. Rev. Lett. **91**, 157002 (2003).
12. M. Büttiker, "The quantum phase of flux correlations in wave-guides", Physica B **175**, 199 - 212, (1991).
13. M. Büttiker, "Flux-sensitive correlations of mutually incoherent quantum channels", Phys. Rev. Lett. **68**, 843 -846, (1992).
14. V. Cerletti, W. A. Coish, O. Gywat, and D. Loss, "Recipes for spin-based quantum computing", (unpublished). cond-mat/0412028
15. M. Blaauboer, and D. P. DiVincenzo, "Detecting entanglement using a double quantum dot turnstile", (unpublished). cond-mat/0502060
16. P. Samuelsson, E.V. Sukhorukov, and M. Büttiker, "Electrical current noise of a beamsplitter as a test of spin entanglement", Phys. Rev. B. **70**, 115330 (2004).
17. O. Sauret, D. Feinberg, and T. Martin, "Quantum master equations for the superconductor-quantum dot entangler", Phys. Rev. B **70**, 245313 (2004).
18. P. Samuelsson, E. V. Sukhorukov, and M. Büttiker, "Two-Particle Aharonov-Bohm Effect and Entanglement in the Electronic Hanbury Brown-Twiss Setup", Phys. Rev. Lett. **92**, 026805 (2004).
19. For a wider context, see also M. Büttiker, P. Samuelsson and E.V. Sukhorukov, "Entangled Hanbury Twiss effects with edge states", Physica E**20**, 33 - 42 (2003).
20. For non-interacting quasi-particles the n-th order current correlation is needed to test n-particle processes. In contrast in the presence of interactions the n-th order current correlation can depend on higher order processes. For this reason it is possible to observe a two-particle Aharonov-Bohm effect even in the (co-tunneling) current (see D. Loss and E. V. Sukhorukov, "Probing Entanglement and Nonlocality of Electrons in a Double-Dot via Transport and Noise", Phys. Rev. Lett. **84**, 1035 -1038 (2000)).
21. R. Hanbury Brown and R. Q. Twiss, "Test of a new type of Stellar Interferometer on Sirius", Nature **178**, 1046 - 1048, (1956).
22. B. Yurke and D. Stoler, "Bell's-inequality experiments using independent-particle sources", Phys. Rev. A **46**, 2229 - 2234, (1992).
23. A similar geometry but for Mach-Zehnder interference has recently been realized, Y. Ji, Y. Chung, D. Sprinzak, M. Heiblum, D. Mahalu, H. Shtrikman, "An electronic Mach-Zehnder interferometer", Nature **422,** 415 -418, (2003).
24. C.W.J. Beenakker, C. Emary, M. Kindermann, and J. L. van Velsen, "Proposal for Production and Detection of Entangled Electron-Hole Pairs in a Degenerate Electron Gas", Phys. Rev. Lett. **91**, 147901 (2003).
25. C.W.J. Beenakker, M. Kindermann, "Quantum Teleportation by Particle-Hole Annihilation in the Fermi Sea", Phys. Rev. Lett. **92**, 056801 (2004).
26. J.F. Clauser, M. A. Horne, A. Shimony, and R. A. Holt, "Proposed Experiment to Test Local Hidden-Variable Theories", Phys. Rev. Lett. **23**, 880 -884, (1969); J.F Clauser and M.A. Horne, "Experimental consequences of objective local theories", Phys. Rev. D **10**, 526 - 535, (1974).
27. X. Maître, W. D. Oliver and Y. Yamamoto, ", "Entanglement in 2DEG systems: towards a detection loophole-free test of Bell's inequality Physica E **6**, 301 -305, (2000); S. Kawabata, "Test of Bell's inequality using the spin filter effect in ferromagnetic semiconductor microstructures", J. Phys. Soc. Jpn. **70**, 1210-1213, (2001).

28. N.M. Chtchelkatchev, G. B. Lesovik, G. Blatter and T. Martin, "Bell inequalities and entanglement in solid-state devices"' Phys. Rev. B **66**, 161320 (2002).
29. A. V. Lebedev, G. B. Lesovik, and G. Blatter, "Entanglement in a noninteracting mesoscopic structure", Phys. Rev. B **71**, 045306 (2005).
30. P. Samuelsson, E. V. Sukhorukov, M. Büttiker, "Orbital entanglement and violation of Bell inequalities in the presence of dephasing", Turk J. Phys. **27**, 481 (2003).
31. J. L. van Velsen, M. Kindermann, C. W. J. Beenakker, "Dephasing of entangled electron-hole pairs in a degenerate electron gas", Turk J. Phys. **27**, 323 (2003).
32. In the single edge state geometry of Fig. (3) the qubit is protected aginst "single-spin flip".
33. L. Faoro, F. Taddei, and R. Fazio, "Clauser-Horne inequality for electron-counting statistics in multiterminal mesoscopic conductors", Phys. Rev. B **69**, 125326 (2004).
34. R. Landauer and M. Büttiker, "Drift and Diffusion in Reversible Computation", Physica Scripta, **T9**, 155 - 164 (1987).
35. P. Samuelsson and M. Büttiker, "Dynamic generation of orbital quasiparticle entanglement in mesoscopic conductors", (unpublished). cond-mat/0410581
36. P.W. Brouwer, "Scattering approach to parametric pumping", Phys. Rev. B **58**, 10135 - 10138, (1998); M. Büttiker, H. Thomas and A. Pretre, "Current partition in multiprobe conductrs in the presence of slowly oscillating external potentials", Z. Phys. B **94**, 133 - 137 (1994); J.E. Avron, A. Elgart, G. M. Graf, and L. Sadun, "Geometry, statistics, and asymptotics of quantum pumps", Phys. Rev. B **62**, 10618 - 10621 (2000).
37. M. Moskalets and M. Büttiker, "Floquet scattering theory of quantum pumps", Phys. Rev. B **66**, 205320 (2002).
38. M. Moskalets and M. Büttiker, "Dissipation and noise in adiabatic quantum pumps", Phys. Rev. B **66**, 035306 (2002); "Floquet scattering theory for current and heat noise in large amplitude adiabatic pumps", Phys. Rev. B **70**, 245305 (2004).
39. J.E Avron, A. Elgart, G. M. Graf, and L. Sadun, "Optimal Quantum Pumps", Phys. Rev. Lett. **87**, 236601 (2001); M.L. Polianski, M.G. Vavilov, P.W. Brouwer, "Noise through quantum pumps", Phys. Rev. B **65**, 245314 (2002); "Quantum pumping and dissipation: From closed to open systems", D. Cohen, Phys. Rev. B **68**, 201303 (2003).
40. L. H. Reydellet, P. Roche, D. C. Glattli, B. Etienne and Y. Jin, "Quantum Partition Noise of Photon-Created Electron-Hole Pairs", Phys. Rev. Lett. **90**, 176803 (2004).
41. In the context of adiabatic pumps electron-hole pairs are discussed by M. Moskalets and M. Büttiker in Refs. [37, 38].
42. C. W. J. Beenakker, Titov and Trauzettel, "Optimal quantum entanglement pump", (unpublished). cond-mat/0502055
43. A. Andreev and A. Kamenev, "Counting Statistics of an Adiabatic Pump", Phys. Rev. Lett. **85**, 1294 (2000); V. Kashcheyevs, A. Aharony, and O. Entin-Wohlman, "Resonance approximation and charge loading and unloading in adiabatic quantum pumping", Phys. Rev. B **69**, 195301 (2004).